Inorganic Chemistry

Article

pubs.acs.org/IC

Ferrocene-*o*-Benzosemiquinonato Tin(IV) Electron-Transfer Complexes

Ekaterina V. Ilyakina,[†] Andrey I. Poddel'sky,*[,†] Georgy K. Fukin,[†] Artem S. Bogomyakov,[‡] Vladimir K. Cherkasov,[†] and Gleb A. Abakumov[†]

[†]G. A. Razuvaev Institute of Organometallic Chemistry, Russian Academy of Sciences, 49 Tropinina str., 603950, Nizhniy Novgorod, GSP-445, Russia

[‡]International Tomography Center, Siberian Branch, Russian Academy of Sciences, 3a Institutskaya Str., 630090, Novosibirsk, Russia

Supporting Information

ABSTRACT: The interaction of ferrocene with tin(IV) *o*-benzosemiquinonato complexes in acetonitrile results in a reversible electron transfer (ET) from ferrocene to the redox-active ligand with the formation of electron-transfer complexes $[(3,6\text{-Cat})SnBr_3]^-[Cp_2Fe]^+$ (**1**) and $[(3,6\text{-Cat})(3,6\text{-SQ})SnCl_2]^-[Cp_2Fe]^+$ (**2**), where 3,6-Cat is the 3,6-di-*tert*-butyl-catecholate dianion and 3,6-SQ is the 3,6-di-*tert*-butyl-*o*-benzosemiquinonato radical anion. The ET process and the solvent effect in the system ≪ferrocene−*o*-benzosemiquinonato tin(IV) complexes≫ were investigated on the basis of a combination of spectroscopic and X-ray diffraction methods. The molecular structures of **1** and **2** were confirmed by X-ray analysis. Complex **2** demonstrates the ferromagnetic coupling in the linear chain alternating ···$D^+{}^\bullet A^-{}^\bullet D^+{}^\bullet A^-{}^\bullet$··· motif.

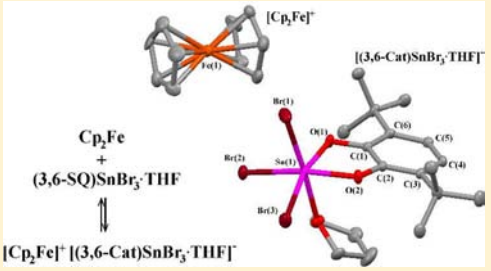

INTRODUCTION

Electron-transfer reactions play an important role in a variety of chemical and biological processes.[1] From this viewpoint, the continuing interest in ferrocene and ferrocene-linked species is focused on their ability to form the electron-transfer systems where the ferrocene moiety acts as an electron donor (D) being combined with the electron acceptor (A);[2] in some cases, this process may be thermally and light induced.[2c,3] Some unusual properties of these systems are associated with $D^+\cdots A^-$ type interactions, e.g., unique magnetic behavior of the first organic magnet $[Fe(C_5Me_5)_2]^+[TCNE]^-$ ($Fe(C_5Me_5)_2$, decamethylferrocene; TCNE, tetracyanoethylene).[4]

Dyads based on the complexes with redox-active quinoid-type ligands (capable of reversible oxidation or reduction in the metal coordination sphere[5]) and ferrocene are proven as a promising system in terms of electron-transfer interactions.[6] However, nontransition metal complexes based on redox-active ligands have never been noticed in such types of processes.

Herein, we report the synthesis and characterization of ferrocene−*o*-benzosemiquinonato tin(IV) electron-transfer complexes $[(3,6\text{-Cat})SnBr_3]^-[Cp_2Fe]^+$ (**1**) and $[(3,6\text{-Cat})(3,6\text{-SQ})SnCl_2]^-[Cp_2Fe]^+$ (**2**).

EXPERIMENTAL SECTION

Materials and Methods. All manipulations on complexes were performed under conditions excluding air oxygen and moisture. Solvents were purified following standard procedures.[7] The initial complexes $(3,6\text{-SQ})SnBr_3\cdot THF$ and $(3,6\text{-SQ})_2SnCl_2$ were obtained using known methods.[8] Ferrocene was the reagent grade.

Infrared spectra of complexes **1**, **2**, and **3** were recorded in the 400−3500 cm^{-1} region on a FSN-1201 spectrophotometer in Nujol mulls and reported in cm^{-1}; the NIR spectrum of complex **2** was recorded in the 800−2500 nm region on a Bruker Vertex 70 spectrophotometer in Nujol mulls. X-band EPR spectra of **2** and **3** were recorded on a Bruker EMX (working frequency ∼9.75 GHz) spectrometer. The g_i values were determined using DPPH as the reference (g_i = 2.0037). The HFS constants were obtained by simulation with the WinEPR SimFonia Software (Bruker), and EasySpin 4.0.0.[9] UV−visible spectra of **1** and **2** were recorded on a Perkin−Elmer Lambda 25 UV−Vis spectrophotometer. The magnetic susceptibility of the polycrystalline sample of **2** was measured with a Quantum Design MPMS*XL* SQUID magnetometer in the temperature range 2−300 K with a magnetic field of up to 5 kOe. Diamagnetic corrections were made using the Pascal constants. The effective magnetic moment was calculated as $\mu_{eff}(T) = [(3k/N_A\mu_B^2)\chi T]^{1/2} \approx (8\chi T)^{1/2}$.

X-Ray Crystallography. Intensity data for **1** and **2** were collected at 100 K on a Smart Apex diffractometer with graphite monochromated Mo Ka radiation (λ = 0.71073 Å) in the $\varphi-\omega$ scan mode (ω = 0.3°, 10 s on each frame). SADABS[10a] was used to perform area-detector scaling and absorption corrections. The structures were solved with the direct method and were refined on F^2 using all reflections with the SHELXTL package.[10b] All non-hydrogen atoms were refined anisotropically. Hydrogen atoms were placed in calculated positions and refined in the "riding-model" (U_{iso}(H) = 1.5U_{eq}(C) in CH_3 groups and U_{iso}(H) = 1.2U_{eq}(C) in other ligands). CCDC-919677 (**1**) and CCDC-919678 (**2**) contain the supplementary crystallographic data for this paper.

Synthesis of Compounds. *$[(3,6\text{-Cat})SnBr_3]^-[Cp_2Fe]^+$ (**1**).* The solution of ferrocene (1 mmol, 0.186 g) in 10 mL of acetonitrile was added to the solution of $(3,6\text{-SQ})SnBr_3\cdot THF$ (1 mmol, 0.651 g) in 20 mL of the same solvent. The color of the reaction mixture turned from dark-green to deep-blue. The solvent was removed at half. The X-ray

Received: January 29, 2013
Published: April 8, 2013

   dx.doi.org/10.1021/ic400713p | *Inorg. Chem.* 2013, 52, 5284−5289

Scheme 1. The Reaction of *o*-Benzosemiquinonato Tin(IV) Halogenides with Ferrocene

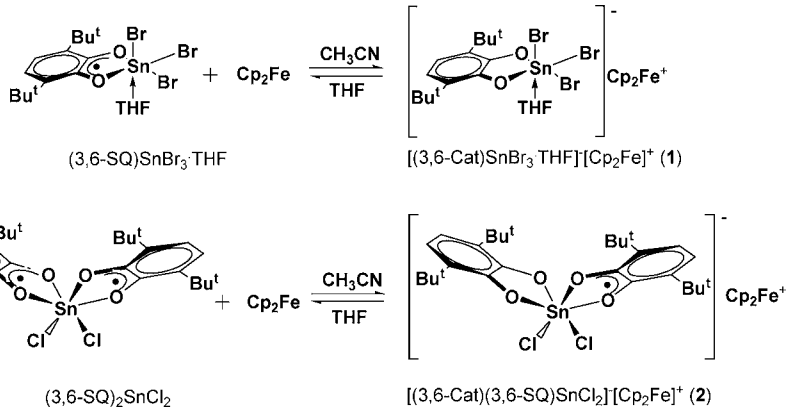

Scheme 2. The Electrochemical Processes for (3,6-SQ)SnBr$_3$·THF and (3,6-SQ)$_2$SnCl$_2$

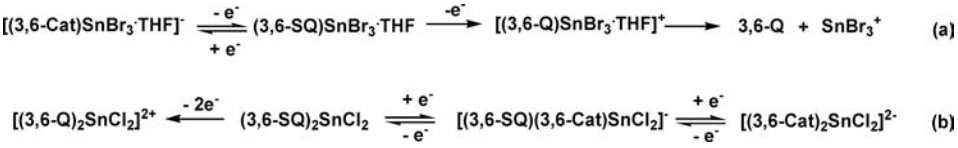

suitable deep-blue crystals of complex **1** were isolated after the storage of solution at −12 °C over 12 h. Complex **1** is sensitive to the air and moisture in solution and stable in the crystalline state. The yield is 0.762 g (91%). Anal. Calcd for $C_{28}H_{38}Br_3FeO_3Sn$: C, 40.19; H, 4.58; Br, 28.64; Fe, 6.67; Sn, 14.19. Found: C, 40.23; H, 4.54; Br, 28.67; Fe, 6.71; Sn, 14.13%. IR (nujol, cm^{-1}): 3098 m, 1581 w, 1482 w, 1417 w, 1394 s, 1350 w, 1290 w, 1281 w, 1257 w, 1238 s, 1208 w, 1200 w, 1148 m, 1116 w, 1074 w, 1025 s, 1013 m, 971 s, 935 s, 918 m, 871 m, 854 s, 841 s, 807 m, 798 m, 695 s, 651 m, 612 w, 600 w, 477 m.

[(3,6-Cat)(3,6-SQ)SnCl$_2$]$^-$[Cp$_2$Fe]$^+$ (**2**). The solution of ferrocene (1 mmol, 0.186 g) in 10 mL of THF was added to the solution of (3,6-SQ)$_2$SnCl$_2$ (1 mmol, 0.630 g) in 20 mL of the same solvent. The solvent was changed with acetonitrile (15 mL). The color of the reaction mixture turned from dark green to deep blue. The X-ray suitable deep-blue crystals of complex **2** were isolated after storage at −12 °C over 12 h. Complex **2** is sensitive to the air and moisture in solution and stable in the crystalline state. The yield is 0.661 g (81%). Anal. Calcd for $C_{38}H_{50}Cl_2FeO_4Sn$: C, 55.91; H, 6.17; Cl, 8.69; Fe, 6.84; Sn, 14.54. Found: C, 56.01; H, 6.18; Cl, 8.73; Fe, 6.82; Sn, 14.51%. IR (nujol, cm^{-1}): 3122 w, 3106 m, 3098 m, 3082 w, 2293 w, 2252 w, 1579 w, 1549 w, 1479 s, 1420 s, 1399 s, 1365 m, 1353 m, 1336 w, 1307 w, 1293 w, 1280 w, 1260 m, 1242 s, 1206 m, 1182 w, 1148 m, 1112 w, 1056 w, 1026 w, 1008 m, 973 s, 967 s, 954 s, 940 m, 932 m, 922 m, 860 s, 851 s, 832 s, 808 m, 792 s, 703 s, 682 s, 652 s, 616 w, 603 w, 565 m, 542 w, 496 m, 485 m.

[(3,6-Cat)(3,6-SQ)SnCl$_2$]$^-$[Cp$_2$Co]$^+$ (**3**). The solution of cobaltocene (1 mmol, 0.189 g) in 10 mL of THF was added to the solution of (3,6-SQ)$_2$SnCl$_2$ (1 mmol, 0.630 g) in 20 mL of the same solvent. The solvent was changed with acetonitrile (15 mL). The color of the reaction mixture turned from dark green to green brown. The microcrystalline green-brown powder of complex **3** was isolated after storage at −12 °C over 12 h. Complex **3** is sensitive to the air and moisture in solution and stable in the crystalline state. The yield is 0.688 g (84%). Anal. Calcd for $C_{38}H_{50}Cl_2CoO_4Sn$: C, 55.70; H, 6.15; Cl, 8.65; Co, 7.19; Sn, 14.49. Found: C, 55.74; H, 6.13; Cl, 8.73; Co, 7.21; Sn, 14.44%. IR (nujol, cm^{-1}): 3110 m, 3103 m, 3085 w, 2296 w, 2250 w, 1580 w, 1547 w, 1484 s, 1425 s, 1415 s, 1399 s, 1354 m, 1336 w, 1308 w, 1291 w, 1280 m, 1258 m, 1241 s, 1206 m, 1111 w, 1065 w, 1028 w, 1007 s, 974 s, 954 s, 939 m, 922 m, 898 w, 868 s, 855 m, 833 m, 807 m, 792 m, 702 s, 683 m, 651 s, 616 w, 605 w, 588 w, 564 m, 544 w, 496 m, 485 w, 457 s.

RESULTS AND DISCUSSION

It was found that the interaction of (3,6-SQ)SnBr$_3$·THF and (3,6-SQ)$_2$SnCl$_2$ with ferrocene in acetonitrile leads to the formation of electron-transfer D$^+$A$^-$ type complexes **1** and **2** accompanied by the reduction of *o*-benzosemiquinonato to the catecholate ligand and the oxidation of ferrocene to the ferrocenium cation (Scheme 1).

The electrochemical investigations for *o*-benzosemiquinonato tin(IV) complexes (3,6-SQ)SnBr$_3$·THF and (3,6-SQ)$_2$SnCl$_2$ have been performed in order to evaluate redox properties of these complexes. Cyclic voltammograms (CVs) were recorded in acetonitrile solutions of complexes containing 0.10 M [Bu$_4$N]ClO$_4$ as a supporting electrolyte at a glassy carbon working electrode and a Ag/AgCl/KCl(sat.) reference electrode. The potentials are referenced versus the ferrocenium/ferrocene couple (Fc$^+$/Fc). Table S1 (see Supporting Information) summarizes these results; the CVs of *o*-benzosemiquinonato tin(IV) complexes are given in Figures S1 and S2, respectively. In accordance with cyclic voltammetry data, the electrochemical reduction of (3,6-SQ)SnBr$_3$·THF is observed in the anodic region; the electrochemical process at 0.14 V has a quasireversible nature and corresponds to the transfer of one electron (Figure S1). The oxidation of (3,6-SQ)SnBr$_3$·THF is the irreversible process observed at 0.83 V and accompanied by the decomposition of the complex with 3,6-di-*tert*-butyl-*o*-benzoquinone decoordination (Scheme 2a). The CV of (3,6-SQ)$_2$SnCl$_2$ (Figure S2) displays two reversible one-electron-transfer waves at 0.09 and −0.22 V corresponding to the formation of mono- and dianionic forms of complex (3,6-SQ)$_2$SnCl$_2$ (Scheme 2b). The oxidation of (3,6-SQ)$_2$SnCl$_2$ is a two-electron irreversible process at 0.81 V, leading to the formation of an unstable dicationic complex.

So, initial *o*-benzosemiquinonato tin(IV) halogenides (3,6-SQ)SnBr$_3$·THF and (3,6-SQ)$_2$SnCl$_2$ possess unusually high redox potentials for such types of complexes: 0.14 and 0.09 V, respectively, vs Cp$_2$Fe/Cp$_2$Fe$^+$. This fact indicates that (3,6-SQ)SnBr$_3$·THF and (3,6-SQ)$_2$SnCl$_2$ are able to demonstrate oxidative abilities toward ferrocenes producing ferrocenium

dx.doi.org/10.1021/ic400713p | *Inorg. Chem.* 2013, 52, 5284−5289

salts, which is surprising because the ferrocenium cation is well-known as an oxidizing agent.[11] Furthermore, in the case of complex $(3,6\text{-SQ})_2SnCl_2$, only one *o*-benzosemiquinonato ligand reduction takes place despite the molar ratio of reagents. The replacement of acetonitrile with THF results in the reversion of the system to the initial state. The solvent effect is caused by the more difficult charge separation in the solvent of lower dielectric capacitivity. The changes in UV−visible spectra well illustrate this solvent effect. Figure 1 shows UV−visible

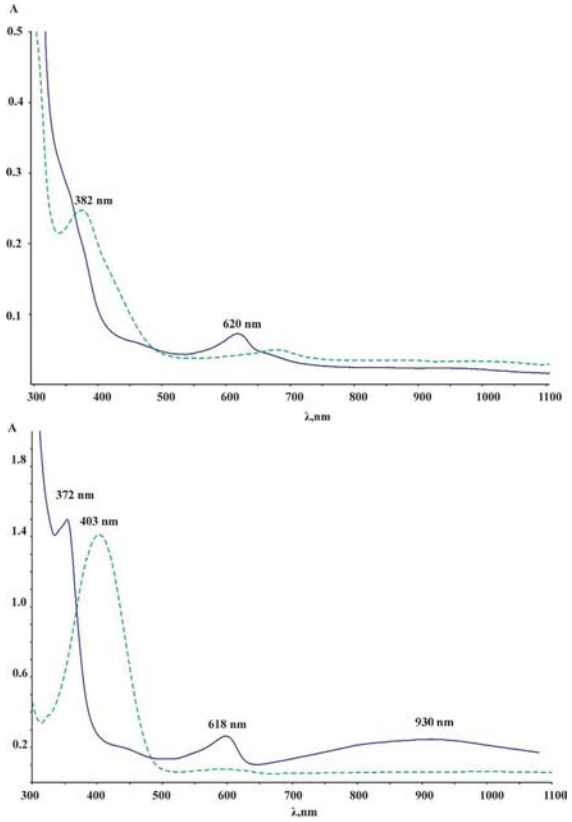

Figure 1. UV−visible spectra of the systems ≪(3,6-SQ)$SnBr_3$·THF + Cp_2Fe≫ (top) and ≪$(3,6\text{-SQ})_2SnCl_2$ + Cp_2Fe≫ (bottom) in THF (dotted line) and acetonitrile (solid line).

spectra of the systems ≪*o*-benzosemiquinonato tin(IV) complex + Cp_2Fe≫ in the different solvents. UV−visible spectra in THF correspond to the superposition of spectra of ferrocene and *o*-benzosemiquinonato complex (3,6-SQ)-$SnBr_3$·THF or $(3,6\text{-SQ})_2SnCl_2$. The replacement of solvent with acetonitrile results in the appearance of new maxima (620 and 618 nm, respectively) which are characteristic for the complexes containing a ferrocenium cation.[12] In addition, the broad *o*-benzosemiquinone−catecholate ligand−ligand charge-transfer band (LLCT) with λ_{max} = 930 nm is observed in the UV−vis spectrum of the complex **2** solution. This charge-transfer band is also detected in NIR in the solid state.

The reduction of *o*-benzosemiquinonato to a catecholato ligand in **1** and **2** is confirmed by the presence of strong intensive bands in the region of 1270−1220 cm^{-1} in IR spectra (Figure S3) which correspond to the stretching vibrations of single C−O bonds of the catecholate ligand.[13]

The catecholato complex **1** is EPR-silent, and its formation in the reaction of (3,6-SQ)$SnBr_3$·THF with ferrocene is accompanied by the disappearance of the EPR spectrum of the initial *o*-benzosemiquinonato complex. On the contrary, complex **2**—a product of interaction of diradical complex $(3,6\text{-SQ})_2SnCl_2$ with ferrocene—contains one *o*-benzosemiquinonato radical anion that is reflected in the appearance of the specific EPR spectrum (Figure 2).

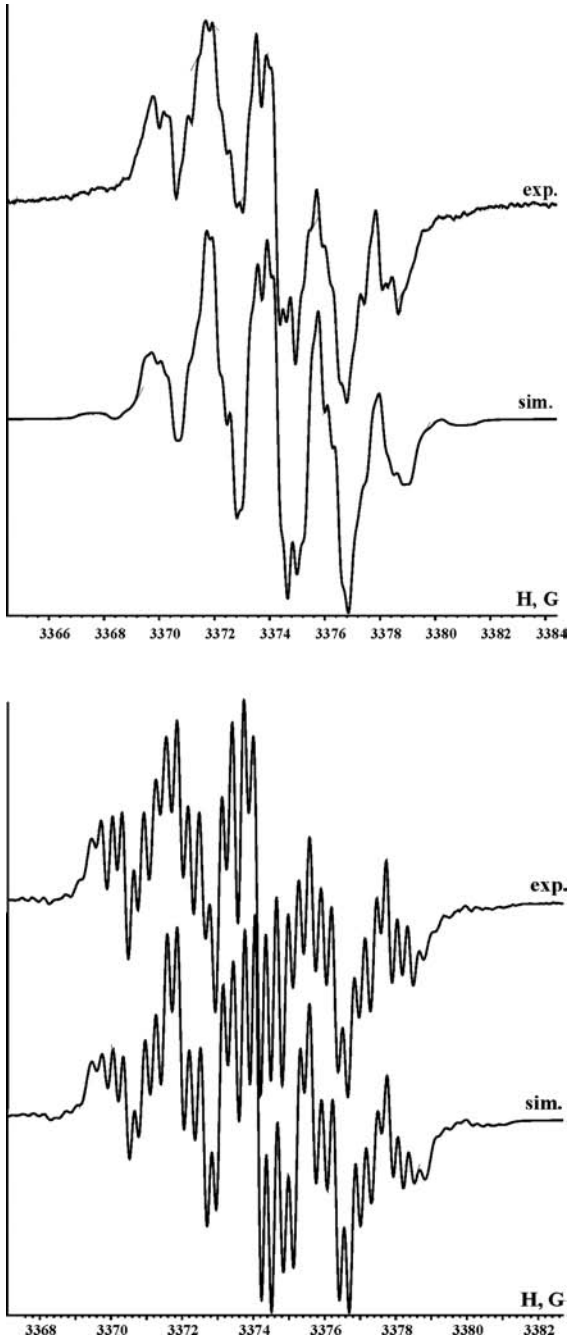

Figure 2. Experimental X-band EPR-spectra (exp.) and their computer simulations (sim.) for complexes **2** (top) and **3** (bottom) (RT, acetonitrile).

The hyperfine structure (HFS) of the EPR spectrum of **2** is caused by the hyperfine coupling of an unpaired electron with two pairs of hydrogen atoms ^1H (99.98%, I = 1/2, μ_N = 2.7928) in the fourth and fifth positions of aromatic rings of both chelating ligands, magnetic nuclei of two chlorine atoms (^{35}Cl, 75.77%, I = 3/2, μ_N = 0.82187 and ^{37}Cl, 24.23%, I = 3/2, μ_N = 0.68412), and the satellite splitting on magnetic tin nuclei

dx.doi.org/10.1021/ic400713p | Inorg. Chem. 2013, 52, 5284−5289

(^{117}Sn, 7.68%, I = 1/2, μ_N = 1.000 and ^{119}Sn, 8.58%, I = 1/2, μ_N = 1.046).[14] The HFS with two pairs of pairwise nonequivalent hydrogens and two chlorine atoms indicates the fast migration of unpaired electron (in the EPR time-scale) between catecholato and *o*-benzosemiquinonato ligands mediated by a tin atom, which is also confirmed by the values of HFS constants $a_i(^1H)$ and $a_i(^{35}Cl)/(^{37}Cl)$, which are nearly two times lower than in corresponding mono-*o*-benzosemiquinonato tin(IV) complexes.[8] The decreasing temperature leads to the lowering of the rate of this process (the slow electron migration between two chelating ligands in the EPR time scale[15]), and the localized structure is observed. However interactions between the monoradical anion and paramagnetic transition metal cation complicate the resolution of the EPR spectrum and the clear determination of HFS constants. In order to simplify the evaluation of HFS constants, the related tin(IV) complex $[(3,6\text{-Cat})(3,6\text{-SQ})SnCl_2]^-[Cp_2Co]^+$ (**3**) containing a diamagnetic cobaltocenium cation was synthesized by the same reaction between $(3,6\text{-SQ})_2SnCl_2$ and cobaltocene. The EPR spectrum of complex **3** is well-resolved and has well-defined HFS constants in contrast to the EPR spectrum of **2**. The values of HFS constants and *g* factors for complexes **2** and **3** are listed in Table 1.

Table 1. The EPR Spectral Data for Complexes 2 and 3

complex	g_i	a_i (^{1}H), G	a_i (^{1}H), G	a_i (^{35}Cl)/a_i (^{37}Cl), G	a_i (^{117}Sn)/ a_i (^{119}Sn), G
2	2.0035	2.21	1.60	0.30/0.25	4.49/4.70
3	2.0035	2.20	1.50	0.30/0.25	4.35/4.55

The crystal structures of complexes **1** and **2** have been determined by single-crystal X-ray crystallography at 100(2) K.

In accordance with X-ray diffraction data, tin(IV) atoms in **1** and **2** have distorted octahedral environments (Figure 3). The C−O distances (C(1)−O(1) is 1.368(4) Å, C(2)−O(2) is 1.359(4) Å) of the chelating ligand in complex **1** lie in the range 1.35−1.37 Å that corresponds to the single C−O distances in such type of ligands and confirms its dianionic catecholate form.[13] Complex **2** adopts a cis configuration, and the dihedral angle between chelating ligands planes is 68.00°. The geometrical features of these ligands confirm their localized radical-anion *o*-benzosemiquinonato form (the C(1)−O(1) and C(2)−O(2) distances are 1.298(4) and 1.287(4) Å and lie in the range 1.29−1.30 Å typical for the one-and-half C−O bonds in *o*-benzosemiquinonato complexes; the quinoid distortion pattern is observed for the six-membered carbon ring C(1−6)) and dianionic catecholate form (the C(7)−O(3) and C(8)−O(4) distances are 1.363(4) and 1.358(4) Å and lie in the range 1.35−1.36 Å that corresponds to the single C−O bonds in catecholates).[8,13,16] The trans influence of chlorine ligands in complex **2** is reflected in the elongation of the corresponding Sn−O bonds (Sn(1)−O(2) and Sn(1)−O(3)). The iron atom of the ferrocenium moiety in both complexes has a prismatic environment, and Fe−C bond lengths confirm the cationic ferrocenium nature.[17] The selected bond lengths and angles for complexes **1** and **2** are collected in Table 2. The crystallographic data and structure refinement details are given in Table S2.

Good support for the assignment of the localized *o*-semiquinonato-catecholato structure of **2** can be given using the calculation of Brown for the "metrical oxidation state."[18] The calculated oxidation states for *o*-benzosemiquinonato and catecholato ligands are −0.97 ± 0.05 (for ring C(1−6)) and −1.91 ± 0.11 (for ring C(7−12)), respectively.

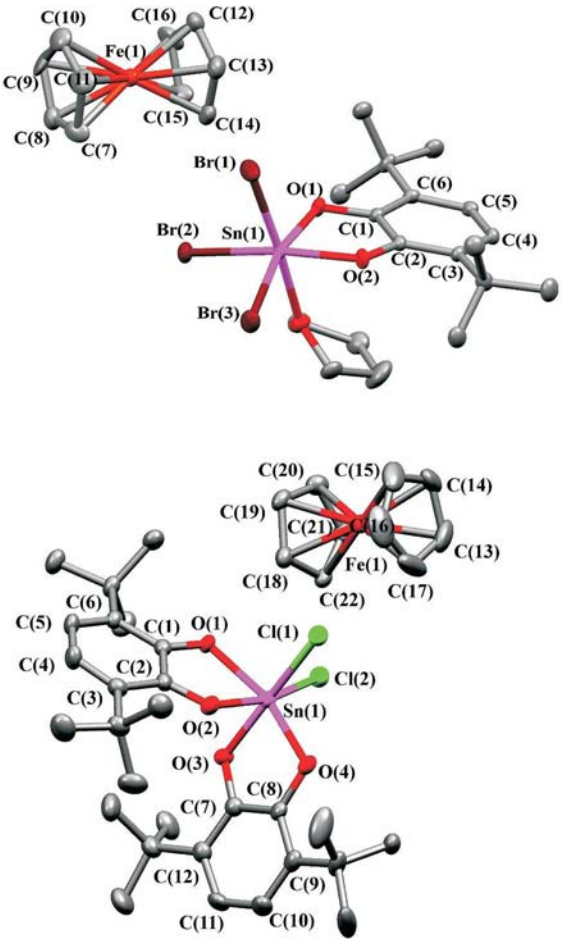

Figure 3. The molecular structures of complexes **1** (top) and **2** (bottom). Ellipsoids of 50% probability; hydrogen atoms are omitted for clarity.

The interesting observations can be done for anion $[(3,6\text{-SQ})(3,6\text{-Cat})SnCl_2]^-$ in complex **2** as a mixed-valence bis(dioxolene) type compound. In the accordance with X-ray structure analysis at 100 K, the anion reveals the localized oxidation state of ligands (SQ and Cat forms) in the solid state. At the same time, the presence of a *o*-benzosemiquinone−catecholate ligand−ligand charge-transfer band (LLCT) with λ_{max} = 930 nm in solution of **2** is consistent with the Robin and Day class II mixed-valence system.[19a] The width of this LLCT band at half-height is ca. 4850 cm^{-1} and $(\Delta\nu_{1/2})^2/\nu_{max}$ = (4850 cm^{-1})^2/10752 cm^{-1} = 2188 cm^{-1}, which is close to 2310 cm^{-1} predicted by the Hush model for class II systems.[1a,19b,c] The calculated value of the electronic coupling parameter H_{AB} between the two redox sites (in cm^{-1}) evaluated by the Mulliken−Hush expression (see Supporting Information) is 740 cm^{-1}.[1a,19b,c] Thus, complex **2** is a class II species in solution according to UV−vis, EPR, and IR spectroscopy.

Miller and Epstein have shown that the electron transfer salt $[Fe(C_5Me_5)_2]^{+\bullet}[TCNE]^{-\bullet}$ containing a paramagnetic ferrocenium cation and tetracyanoethylene anion demonstrates ferromagnetic behavior.[4] The authors have shown that substantial cooperative magnetic interactions may be observed in donor−acceptor systems of the DADA type when both donor D and acceptor A are radicals with S = 1/2. In complex

dx.doi.org/10.1021/ic400713p | Inorg. Chem. 2013, 52, 5284−5289

Table 2. The Selected Bond Lengths and Angles for Complexes 1 and 2

bond length, Å	1	bond length, Å	2
Sn(1)−O(1)	2.032(2)	Sn(1)−O(1)	2.099(2)
Sn(1)−O(2)	2.041(2)	Sn(1)−O(2)	2.142(2)
Sn(1)−Br(1)	2.5308(5)	Sn(1)−O(3)	2.031(2)
Sn(1)−Br(2)	2.5483(4)	Sn(1)−O(4)	2.005(2)
Sn(1)−Br(3)	2.5504(5)	Sn(1)−Cl(1)	2.3873(9)
C(1)−O(1)	1.368(4)	Sn(1)−Cl(2)	2.3934(8)
C(2)−O(2)	1.359(4)	C(1)−O(1)	1.298(4)
C(1)−C(2)	1.419(5)	C(2)−O(2)	1.287(4)
C(2)−C(3)	1.409(5)	C(7)−O(3)	1.363(4)
C(3)−C(4)	1.392(5)	C(8)−O(4)	1.358(4)
C(4)−C(5)	1.395(5)	C(1)−C(2)	1.466(4)
C(5)−C(6)	1.392(5)	C(1)−C(6)	1.425(4)
C(1)−C(6)	1.409(5)	C(2)−C(3)	1.434(5)
C(7)−Fe(1)	2.070(6)	C(3)−C(4)	1.366(5)
C(8)−Fe(1)	2.082(6)	C(4)−C(5)	1.433(5)
C(9)−Fe(1)	2.099(6)	C(5)−C(6)	1.369(4)
C(10)−Fe(1)	2.105(6)	C(7)−C(8)	1.420(4)
C(11)−Fe(1)	2.065(6)	C(7)−C(12)	1.401(5)
C(12)−Fe(1)	2.079(6)	C(8)−C(9)	1.410(4)
C(13)−Fe(1)	2.050(6)	C(9)−C(10)	1.386(5)
C(14)−Fe(1)	2.087(6)	C(10)−C(11)	1.385(5)
C(15)−Fe(1)	2.075(6)	C(11)−C(12)	1.397(5)
C(16)−Fe(1)	2.092(6)	C(13)−Fe(1)	2.083(4)
C(7)−C(8)	1.375(8)	C(14)−Fe(1)	2.085(4)
C(8)−C(9)	1.403(9)	C(15)−Fe(1)	2.086(4)
C(9)−C(10)	1.420(9)	C(16)−Fe(1)	2.063(4)
C(10)−C(11)	1.419(9)	C(17)−Fe(1)	2.080(4)
C(11)−C(7)	1.462(9)	C(18)−Fe(1)	2.083(3)
C(12)−C(13)	1.402(8)	C(19)−Fe(1)	2.109(3)
C(13)−C(14)	1.462(9)	C(20)−Fe(1)	2.110(3)
C(14)−C(15)	1.396(9)	C(21)−Fe(1)	2.074(4)
C(15)−C(16)	1.398(9)	C(22)−Fe(1)	2.060(3)
C(16)−C(12)	1.407(9)	C(13)−C(14)	1.407(6)
		C(14)−C(15)	1.374(6)
		C(15)−C(16)	1.353(7)
		C(16)−C(17)	1.395(7)
		C(17)−C(13)	1.421(7)
		C(18)−C(19)	1.414(5)
		C(19)−C(20)	1.406(5)
		C(20)−C(21)	1.430(5)
		C(21)−C(22)	1.404(5)
		C(22)−C(18)	1.435(5)
angle, deg		angle, deg	
O(2)−Sn(1)−O(1)	81.40(9)	O(1)−Sn(1)−O(2)	76.33(9)
O(2)−Sn(1)−Br(2)	165.82(7)	O(1)−Sn(1)−O(3)	86.84(9)
O(1)−Sn(1)−Br(3)	165.96(7)	O(1)−Sn(1)−O(4)	162.97(9)
Br(2)−Sn(1)−Br(3)	95.630(16)	O(2)−Sn(1)−O(3)	86.91(9)
		O(3)−Sn(1)−O(4)	82.13(9)
		Cl(1)−Sn(1)−Cl(2)	91.74(3)

2, both ferrocenium and the *o*-benzosemiquinonato−catecholato tin(IV) anion are paramagnetic centers with $S = 1/2$. So, one can expect the same magnetic behavior in **2** as that in $[Fe(C_5Me_5)_2]^{+\bullet}[TCNE]^{-\bullet}$. The temperature dependences of the effective magnetic moment (μ_{eff}) and reciprocal magnetic susceptibility ($1/\chi$) for **2** are presented in Figure 4.

At 300 K, the μ_{eff} value is 3.15 μ_B and changes slightly with lowering temperature down to 60 K and below 60 K μ_{eff} increases to 3.69 μ_B at 5 K. The dependence $1/\chi(T)$ obeys

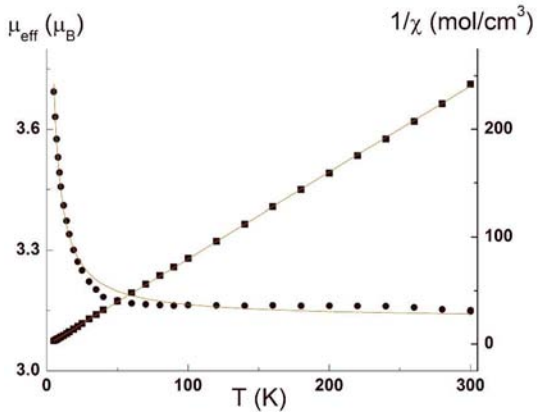

Figure 4. Dependences $\mu_{eff}(T)$ (●) and $\chi^{-1}(T)$ (■) for complex **2** (solid lines − theoretical curves).

Curie−Weiss law with optimal parameters $C = 1.24$ (±0.01) K·cm^3/mol and $\theta = 1.4$ (±0.2) K. The Curie constant C and μ_{eff} (at 300 K) values are higher than the theoretical spin only values for two uncoupled spins with $S = 1/2$ at $g = 2$. The high values are in good agreement with previous results (e.g., for the charge transfer salt $[Fe(C_5Me_5)_2]^{+\bullet}[TCNE]^{-\bullet}$ $\mu_{eff} = 3.1$ μ_B at 300 K).[4] For low spin $[Fe(C_5H_5)_2]^{+\bullet}$ in complexes, μ_{eff} values range from ∼2.3 to ∼2.6 μ_B due to a significant orbital contribution to the magnetic moment.[20] The experimental μ_{eff} value at 300 K corresponds to 2.63 μ_B for $[Fe(C_5H_5)_2]^{\bullet+}$ in assumption that for the tin(IV) complex anion $S = 1/2$ and $g = 2$. The increasing μ_{eff} with lowering temperature and a positive Weiss constant value point to a presence of ferromagnetic coupling between spins of paramagnetic centers. The ferromagnetic chain model was used for the estimation of coupling energy and the best fit parameters J/k and g are 1.08 (±0.04) K and 2.56 (±0.01) (Hamiltonian $H = \Sigma - 2JS_iS_{i+1}$). Thus, the magnetic behavior of charge transfer complex **2** is in good agreement with the conclusions of Miller about the necessity of having both the D and A radicals for stabilizing ferromagnetic coupling in the linear chain $\cdots D^{+\bullet}A^{-\bullet}D^{+\bullet}A^{-\bullet}\cdots$ motif.

■ CONCLUSION

In summary, the first examples of electron-transfer systems containing ferrocene and a nontransition metal complex based on redox-active ligands (ferrocene−*o*-benzosemiquinonato tin(IV) complexes $[(3,6\text{-Cat})SnBr_3]^-[Cp_2Fe]^+$ (**1**) and $[(3,6\text{-Cat})(3,6\text{-SQ})SnCl_2]^-[Cp_2Fe]^+$ (**2**)) are reported. Importantly, that interaction between ferrocene and *o*-benzosemiquinonato tin(IV) halides depends on the solvent media. The fast migration of the unpaired electron between *o*-benzosemiquinonato and catecholato ligands in mixed-ligand complex $[(3,6\text{-Cat})(3,6\text{-SQ})SnCl_2]^-[Cp_2Fe]^+$ in solution was observed. Compound **2** contains a ferrocenium radical cation ($D^{+\bullet}$) and a tin(IV) complex radical anion ($A^{-\bullet}$) and demonstrates the ferromagnetic coupling in the linear chain alternating $\cdots D^{+\bullet}A^{-\bullet}D^{+\bullet}A^{-\bullet}\cdots$ motif. Overall, the further investigations of $D^+\cdots A^-$ interactions in such type systems containing a ferrocenium cation and radical-anion ligand complexes are expected to reveal new promising results.

dx.doi.org/10.1021/ic400713p | Inorg. Chem. 2013, 52, 5284−5289

■ ASSOCIATED CONTENT

Supporting Information

Table S1 containing redox potentials of tin(IV) complexes, Table S2 containing crystallographic data and structure refinement details, Figures S1−S3 containing cyclic voltammogram of tin(IV) complexes and IR spectra, and the details of the electronic coupling parameter H_{AB} calculation are included, as well as CIF and CDX files. This material is available free of charge via the Internet at http://pubs.acs.org.

■ AUTHOR INFORMATION

Corresponding Author

*E-mail: aip@iomc.ras.ru.

Notes

The authors declare no competing financial interest.

■ ACKNOWLEDGMENTS

The electrochemical investigations were performed by Ph.D. Ivan V. Smolyaninov and Prof. Nadezhda T. Berberova (Astrakhan State Technical University, Astrakhan, Russia). We are grateful to RFBR (N 2013-3-01022 and 13-03-00891), President of Russian Federation (Grants NSh-1113.2012.3), for the financial support of this work. This work was performed according to FSP "Scientific and scientific-pedagogical cadres of innovation Russia" for the years 2009−2013 (N8465 from 31.08.2012).

■ REFERENCES

(1) (a) *Electron Transfer in Chemistry*; Balzani, V., Ed.; Wiley-VCH: Weinheim, Germany, 2001; Vols. *1*−*5*. (b) Armstrong, F. A.; Kaim, W.; Schwederski, B. *Bioinorganic Chemistry: Inorganic Chemistry in the Chemistry of Life*; Oxford University: Oxford, U. K., 1995.

(2) (a) Rosenblum, M.; Fish, R. W.; Bennett, C. *J. Am. Chem. Soc.* **1964**, *86*, 5166−5170. (b) Brandon, R. L.; Osiecki, J. H.; Ottenberg, A. *J. Org. Chem.* **1966**, *31*, 1214−1217. (c) Fukuzumi, S.; Yoshida, Y.; Okamoto, K.; Imahori, H.; Araki, Y.; Ito, O. *J. Am. Chem. Soc.* **2002**, *124*, 6794−6795. (d) Fukuzumi, S.; Okamoto, K.; Yoshida, Y.; Imahori, H.; Araki, Y.; Ito, O. *J. Am. Chem. Soc.* **2003**, *125*, 7014−7021. (e) Sporer, C.; Ratera, I.; Ruiz-Molina, D.; Gancedo, J. V.; Ventosa, N.; Wurst, K.; Jaitner, P.; Rovira, C.; Veciana, J. *Solid State Science* **2009**, *11*, 786−792.

(3) (a) Ratera, I.; Ruiz-Molina, D.; Renz, F.; Ensling, J.; Wurst, K.; Rovira, C.; Gutlich, P.; Veciana, J. *J. Am. Chem. Soc.* **2003**, *125*, 1462−1463. (b) Gonzalez-Rodrıguez, D.; Torres, T.; Olmstead, M. M.; Rivera, J.; Herranz, M. A.; Echegoyen, L.; Castellanos, C. A.; Guldi, D. M. *J. Am. Chem. Soc.* **2006**, *128*, 10680−10681.

(4) (a) Miller, J. S.; Epstein, A. J. *Angew. Chem., Int. Ed.* **1994**, *33*, 385−415. (b) Miller, J. S.; Epstein, A. J. *Coord. Chem. Rev.* **2000**, *206*−*207*, 651−660. (c) Miller, J. S. *Dalton Trans.* **2006**, 2742−2749.

(5) (a) Pierpont, C. G.; Lange, C. W. *Prog. Inorg. Chem.* **1994**, *41*, 331−442. (b) Pierpont, C. G. *Coord. Chem. Rev.* **2001**, *219*−*221*, 415−433. (c) Zanello, P.; Corsini, M. *Coord. Chem. Rev.* **2006**, *250*, 2000−2022. (d) Abakumov, G. A.; Nevodchikov, V. I.; Cherkasov, V. K. *Dokl. Akad. Nauk SSSR* **1984**, *278*, 641−645. (e) Shultz, D. A.; Kumar, K. *J. Am. Chem. Soc.* **2001**, *123*, 6431−6432.

(6) (a) Chang, H.-C.; Miyasaka, H.; Kitagawa, S. *Inorg. Chem.* **2001**, *40*, 146−156. (b) Heinze, K.; Reinhardt, S. *Organometallics* **2007**, *26*, 5406−5414.

(7) Perrin, D. D.; Armarego, W. L. F.; Perrin, D. R. *Purification of Laboratory Chemicals*; Pergamon: Oxford, U. K., 1980.

(8) (a) Ilyakina, E. V.; Poddel'sky, A. I.; Piskunov, A. V.; Somov, N. V. *Inorg. Chim. Acta* **2012**, *380*, 57−64. (b) Ilyakina, E. V.; Poddel'sky, A. I.; Piskunov, A. V.; Somov, N. V.; Abakumov, G. A.; Cherkasov, V. K. *Inorg. Chim. Acta* **2013**, *394*, 282−288.

(9) Stoll, S.; Schweiger, A. *J. Magn. Reson.* **2006**, *178*, 42−55.

(10) (a) Sheldrick, G. M. *SADABS*, v.2.01; Bruker AXS: Madison, WI, 1998. (b) Sheldrick, G. M. *SHELXTL*, v. 6.12; Bruker AXS: Madison, WI, 2000.

(11) Connelly, N. G.; Geiger, W. E. *Chem. Rev.* **1996**, *96*, 877−910.

(12) (a) Lee, S.; Bakac, A.; Espenson, J. H. *Inorg. Chem.* **1989**, *28*, 1367−1369. (b) Santiago, M. B.; Declet-Flores, C.; Díaz, A.; Velez, M. M.; Bosques, M. Z.; Sanakis, Y.; Colon, J. L. *Langmuir* **2007**, *23*, 7810−7817. (c) Kumar, P. S.; Kumar, S.; Lakshminarayanan, V. *J. Phys. Chem. B* **2008**, *112*, 4865−4869.

(13) (a) Piskunov, A. V.; Lado, A. V.; Fukin, G. K.; Baranov, E. V.; Abakumova, L. G.; Cherkasov, V. K.; Abakumov, G. A. *Heteroat. Chem.* **2006**, *17*, 481−490. (b) Piskunov, A. V.; Lado, A. V.; Ilyakina, E. V.; Fukin, G. K.; Baranov, E. V.; Cherkasov, V. K.; Abakumov, G. A. *J. Organomet. Chem.* **2008**, *693*, 128−134. (c) Lado, A. V.; Poddel'sky, A. I.; Piskunov, A. V.; Fukin, G. K.; Baranov, E. V.; Ikorskii, V. N.; Cherkasov, V. K.; Abakumov, G. A. *Inorg. Chim. Acta* **2005**, *358*, 4443−4450.

(14) Emsley, J. *The Elements*; Pergamon Press: Oxford, U. K., 1999; p 350.

(15) Kabachnik, M. I.; Bubnov, N. N.; Prokof'ev, A. I.; Solodovnikov, S. P. *Sci. Rev. Ser. B* **1981**, *3* (XXIV, N 22), 197−297.

(16) Batsanov, A. S.; Howard, J. A. K.; Brown, M. A.; McGarvey, B. R.; Tuck, D. G. *Chem. Commun.* **1997**, 699−700.

(17) (a) Webb, R. J.; Lowery, M. D.; Shiomi, Y.; Sorai, M.; Wittebort, R. J.; Hendrickson, D. N. *Inorg. Chem.* **1992**, *31*, 5211−5219. (b) Bradley, S.; Camm, K. D.; Liu, X.; McGowan, P. C.; Mumtaz, R.; Oughton, K. A.; Podesta, T. J.; Thornton-Pett, M. *Inorg. Chem.* **2002**, *41*, 715−726.

(18) Brown, S. N. *Inorg. Chem.* **2012**, *51*, 1251−1260.

(19) (a) Robin, M. B.; Day, P. *Adv. Inorg. Chem. Radiochem.* **1967**, *10*, 247. (b) Hush, N. S. *Prog. Inorg. Chem.* **1967**, *8*, 391−444. (c) Brunschwig, B. S.; Sutin, N. *Coord. Chem. Rev.* **1999**, *187*, 233−254.

(20) (a) Hendrickson, D. N.; Sohn, Y. S.; Gray, G. B. *Inorg. Chem.* **1971**, *10*, 1559−1563. (b) Morrison, W. H.; Krogsrud, S.; Hendrickson, D. N. *Inorg. Chem.* **1973**, *12*, 1998−2004. (c) Morrison, W. H., Jr.; Hendrickson, D. N. *Inorg. Chem.* **1975**, *14*, 2331−2346.